HHS Public Access

Author manuscript

*Mol Cancer Ther*. Author manuscript; available in PMC 2015 December 01.

Published in final edited form as:

*Mol Cancer Ther*. 2014 December ; 13(12): 2876–2885. doi:10.1158/1535-7163.MCT-14-0074.

# Therapeutic Silencing of KRAS using Systemically Delivered siRNAs

**Chad V. Pecot**[1,*], **Sherry Y. Wu**[2], **Seth Bellister**[3], **Justyna Filant**[2], **Rajesha Rupaimoole**[2], **Takeshi Hisamatsu**[2], **Rajat Bhattacharya**[3], **Anshumaan Maharaj**[4], **Salma Azam**[5], **Cristian Rodriguez-Aguayo**[6,7], **Archana S. Nagaraja**[2], **Maria Pia Morelli**[8], **Kshipra M. Gharpure**[2], **Trent A. Waugh**[9], **Vianey Gonzalez-Villasana**[6], **Behrouz Zand**[2], **Heather J. Dalton**[2], **Scott Kopetz**[8], **Gabriel Lopez-Berestein**[6,7,10], **Lee M. Ellis**[3], and **Anil K. Sood**[2,6,10]

[1]Division of Cancer Medicine, The University of Texas MD Anderson Cancer Center, Houston, Texas, USA

[2]Department of Gynecologic Oncology, The University of Texas MD Anderson Cancer Center, Houston, Texas, USA

[3]Department of Surgical Oncology, The University of Texas MD Anderson Cancer Center, Houston, Texas, USA

[4]The University of Texas, Austin, TX, USA

[5]University of North Carolina, Curriculum in Genetics and Molecular Biology, Chapel Hill, NC

[6]Department of Cancer Biology, The University of Texas MD Anderson Cancer Center, Houston, Texas, USA

[7]Department of Experimental Therapeutics, The University of Texas MD Anderson Cancer Center, Houston, Texas, USA

[8]Department of Gastrointestinal Medical Oncology, The University of Texas MD Anderson Cancer Center, Houston, Texas, USA

[9]University of North Carolina, Lineberger Comprehensive Cancer Center, Chapel Hill, NC, USA

[10]Center for RNA Interference and Non-Coding RNA, The University of Texas MD Anderson Cancer Center, Houston, Texas, USA

## Abstract

Despite being amongst the most common oncogenes in human cancer, to date there are no effective clinical options for inhibiting KRAS activity. We investigated whether systemically delivered KRAS siRNAs have therapeutic potential in KRAS mutated cancer models. We identified KRAS siRNA sequences with notable potency in knocking-down KRAS expression. Using lung and colon adenocarcinoma cell lines, we assessed anti-proliferative effects of KRAS

Correspondence should be addressed to A.K.S. (asood@mdanderson.org), The University of Texas MD Anderson Cancer Center, Unit 1362, PO Box 301439, Houston, TX 77230-1439.

*Current Address, Chad V. Pecot, University of North Carolina Lineberger Comprehensive Cancer Center, Department of Medicine, Chapel Hill, North Carolina

**Conflict of interest statement:** The authors report not conflict of interest.

silencing *in vitro*. For *in vivo* experiments, we used a nano-liposomal delivery platform, DOPC, for systemic delivery of siRNAs. Various lung and colon cancer models were utilized to determine efficacy of systemic KRAS siRNA based on tumor growth, development of metastasis and downstream signaling. KRAS siRNA sequences induced >90% knock-down of KRAS expression, significantly reducing viability in mutant cell lines. In the lung cancer model, KRAS siRNA treatment demonstrated significant reductions in primary tumor growth and distant metastatic disease, while the addition of CDDP was not additive. Significant reductions in Ki-67 indices were seen in all treatment groups, while significant increases in caspase-3 activity was only seen in the CDDP treatment groups. In the colon cancer model, KRAS siRNA reduced tumor KRAS and pERK expression. KRAS siRNAs significantly reduced HCP1 subcutaneous tumor growth, as well as outgrowth of liver metastases. Our studies demonstrate a proof-of-concept approach to therapeutic KRAS targeting using nanoparticle delivery of siRNA. This study highlights the potential translational impact of therapeutic RNA interference, which may have broad applications in oncology, especially for traditional “undruggable” targets.

## Introduction

Since its discovery over 30 years ago(1, 2), the KRAS proto-oncogene has remained the single most elusive cancer target. Despite the vast heterogeneity of all malignancies, mutational activation of the RAS GTPases (HRAS, NRAS and KRAS) are present in approximately a third of all cancers(3). While these small monomeric GTPases are part of a superfamily of more than 150 members, direct mutation of other members is rare(4). Typically, RAS activation is catalyzed by guanine nucleotide exchange factors (GEFs) to a GTP-bound state, and subsequently hydrolyzed by GTPase-activating proteins (GAPs) to its inactive, GDP-bound state. However, KRAS missense mutations in codons 12, 13, or 61 sterically interfere with GAP hydrolysis, leading to constitutive activation and promotion of many cancer hallmarks, such as cellular proliferation, survival, cytoskeletal reorganization, and motility(5). While valiant attempts have been made to develop pharmaceutical inhibitors of mutant KRAS-driven cancers, KRAS itself is still widely regarded as ‘undruggable’.

Since the first report of RNA interference (RNAi) in 1998 (6), there has been an explosion in efforts to utilize such a strategy for therapeutic gain(7). Therapeutic RNAi is especially attractive because it enables silencing of cancer molecular targets that otherwise may not be inhibited using conventional approaches. While competitive ATP kinase inhibitors (e.g., imatinib) or monoclonal antibodies (e.g., trastuzumab) have revolutionized treatment of some cancers(8, 9), the lack of such success in KRAS targeting prompted us to investigate whether RNAi has therapeutic potential for drug development. Here, we report a proof-of-concept study in lung and colon cancer preclinical models that demonstrates the efficacy of KRAS silencing using nanoparticle-mediated siRNA delivery. Additionally, we demonstrate in several models that KRAS silencing *in vivo* can potently inhibit development of metastatic disease, the cause of death in approximately 90% of cancer patients(10).

## Materials and Methods

### Cell lines, maintenance and transfection reagents

All cell lines were maintained in 5% CO2/95% air at 37°C. Lung (A549 and H1299) and ovarian (RMUG-S) cells were obtained by the ATCC and maintained in RPMI 1640 supplemented with 10% fetal bovine serum (FBS) and 0.1% gentamicin sulfate (GeminiBioproducts, Calabasas, CA). The A549-Luciferase cell line was made following stable transduction with lenti-virus carrying the luciferase gene (the lentiviral vector was kindly provided by Craig Logsdon's lab). The HCP1 colon cell lines were obtained from a human-derived xenograft model at the M.D. Anderson Cancer Center under an IRB approved protocol as recently described(11). Cell lines were routinely tested to confirm the absence of *Mycoplasma*, and all in vitro experiments were conducted with 60-80% confluent cultures. All cells were reverse-transfected with RNAiMax reagent (Invitrogen) using siRNA molecules (Sigma) at a final concentration of 10-20 nM. Media was changed 4 hours following transfections to minimize toxicity. The siRNA sequences used for KRAS siRNA experiments are as follows:

Negative Control: Sense-UUCUCCGAACGUGUCACGU

Anti-sense-ACGUGACACGUUCGGAGAA

Seq #1: Sense-GUGCAAUGAAGGGACCAGUA,

Anti-sense-UACUGGUCCCUCAUUGCAC

Seq #2: Sense-GUCUCUUGGAUAUUCUCGA,

Anti-sense-UCGAGAAUAUCCAAGAGAC

Seq #3: Sense-CAGCUAAUUCAGAAUCAUU,

Anti-sense-AAUGAUUCUGAAUUAGCUG

### Animals, *in vivo* models and tissue processing

Female athymic nude mice were purchased from the National Cancer Institute, Frederick Cancer Research and Development Center (Frederick, MD). These animals were cared for according to guidelines set forth by the American Association for Accreditation of Laboratory Animal Care and the U.S. Public Health Service policy on Human Care and Use of Laboratory Animals. All mouse studies were approved and supervised by the M.D. Anderson Cancer Center Institutional Animal Care and Use Committee. All animals used were between 8-12 weeks of age at the time of injection. For all animal experiments, cells were trypsinized, washed and resuspended in Hanks' balanced salt solution (HBSS; Gibco, Carlsbad, CA) prior to injection. For the orthotopic lung cancer model, A549-Luc cells were injected by an intra-pulmonary technique [$7.5\times10^5$ in 100 μL 1:1 mixture of HBSS and BD Matrigel (BD Biosciences)] as previously described(12). For the intra-pulmonary injections, mice were anesthetized with ketamine + xylazine and placed in the right lateral decubitus position. Following skin cleaning with an alcohol swab, an incision parallel to the rib cage between ribs 10-11 was made to visualize the lung through the thorax. A 1 mL tuberculin syringe with a 30-g needle was used to inject the cell suspension directly into the lung

parenchyma at the left lateral dorsal axillary line. After injection the incision was closed using surgery clips and the mice were turned on the left lateral decubitus until fully recovered.

For both colon cancer models, $2.5\times10^5$ HCP1 cells per mouse 100 μL HBSS were either injected subcutaneously or intra-splenic (experimental liver metastases model). In the liver metastases model, mice were anesthetized under isofluorane for splenic isolation and cell line injection (day 1), as well as the following day after injection (day 2) in order to perform splenectomy(11). Treatment continued until mice in any group became moribund (approximately 3 weeks).

For the A549 xenograft time-kinetic experiment used to assess for KRAS knock-down following siRNA delivery, $2.5\times10^6$ A549 parental cells were injected subcutaneously into athymic nude mice. Mice were randomly assigned to receive either NC siRNA or the combination of KRAS siRNAs Seq #2 and #3 (150 μg siRNA/kg/mouse). After 4 weeks of cell line injection, siRNAs packed in DOPC nanoliposomes were delivered intra-peritoneally and one tumor per group was obtained at 24, 48 and 96 hours following a single delivery.

For all therapeutic experiments, mice were randomly divided and assigned to their respective treatment groups (n=10 mice/group). A dose of 150 μg siRNA/kg/mouse was packaged within DOPC nanoliposomes and delivered intra-peritoneally at twice weekly intervals as previously described(13). For the A549 lung cancer model, treatment began 10 days after cell line injection and continued for approximately 4 weeks. A 160 μg dose of pharmaceutical grade cisplatin (CDDP; 1 mg/mL concentration) was administered to respective groups once weekly intra-peritoneally. Weekly imaging was performed using the Xenogen IVIS 200 system within 10 minutes following injection of D-Luciferin (150 μg/mL). Living image 2.5 software was used to determine the regions of interest (ROI) and average photon radiance [p/s/$cm^2$/sr] was measured for each mouse.

For the subcutaneous colon cancer model, tumors were monitored until they measured approximately 100 $mm^3$, as determined using the following formula: volume=[LxWxW]/2, where L equals the greatest dimension of the tumor and W equals the perpendicular measurement of the tumor. Twice weekly treatment began once tumors measured approximately 100 $mm^3$ and continued until tumors in any group were approximately 15 mm in any dimension. In the time-kinetic experiment, 2 weeks following HCP1 cell line injection into a total of 4 mice, mice were randomly assigned to receive either NC siRNA-DOPC or KRAS siRNA (Seq #3)-DOPC. After a single injection, mice in each group were sacrificed and tumors were snap frozen at 48 and 96 hours following the injection.

In all experiments, once mice in any group became moribund they were all sacrificed, necropsied, and tumors were harvested. Tumor weights, number and location of tumor nodules were recorded. In the A549 orthotopic lung cancer model, tumor volume was determined using calipers as follows: volume=[LxWxW]/2, where L equals the greatest dimension of the tumor and W equals the perpendicular measurement of the tumor. Tumor

tissue was either fixed in formalin for paraffin embedding, frozen in optimal cutting temperature (OCT) media to prepare frozen slides, or snap frozen for lysate preparation.

### Liposomal nanoparticle preparation

siRNA for *in vivo* intra-tumor delivery was incorporated into DOPC. DOPC and siRNA were mixed in the presence of excess tertiary butanol at a ratio of 1:10 (w/w) siRNA/DOPC (Supplementary Fig. 1). Tween 20 was added to the mixture in a ratio of 1:19 Tween 20:siRNA/DOPC. The mixture was vortexed, frozen in an acetone/dry ice bath and lyophilized. Before *in vivo* administration, this preparation was hydrated with PBS at room temperature at a concentration of 150 μg siRNA/kg per injection (each mouse received 200 μL of DOPC:siRNA:PBS solution by the intra-peritoneal route).

### Immunoblotting

Lysates from cultured cells were prepared using modified RIPA buffer (50 mM Tris–HCl [pH 7.4], 150 mM NaCl, 1% Triton, 0.5% deoxycholate) plus 25 μg/mL leupeptin, 10 μg/mL aprotinin, 2 mM EDTA, and 1 mM sodium orthovana. To prepare lysates of snap-frozen tissue from mice, approximately 30-$mm^3$ cuts of tissue were disrupted with a tissue homogenizer and centrifuged at 13,000 rpm for 30 min within modified RIPA buffer. The protein concentrations were determined using a BCA Protein Assay Reagent kit (Pierce Biotechnology, Rockford, IL). Lysates (100 μg/lane) were loaded and separated on 8% sodium dodecyl sulfate—polyacrylamide gels. Proteins were transferred to a nitrocellulose membrane by semidry electrophoresis (Bio-Rad Laboratories, Hercules, CA) overnight, blocked with 5% milk for 1 hour and then incubated at 4°C with primary antibody [KRAS, 1:500, Abcam ab81075 (cell lysates); KRAS, 1:500, Santa Cruz SC-30 (tumor lysates); pERK1/2, 1:1000, Cell Signaling (4695); ERK1/2, 1:1000, Cell Signaling (4376); pMEK1/2, 1:1000, Cell Signaling (2338); MEK1/2, 1:1000, Cell Signaling (4694); Vinculin, 1:1000, Santa Cruz SC-25336] overnight. After washing with TBST, the membranes were incubated with horseradish peroxidase (HRP)—conjugated horse anti-mouse IgG (1:2000, GE Healthcare, UK) for 2 hours. HRP was visualized by use of an enhanced chemiluminescence detection kit (Pierce). To confirm equal sample loading, the blots were probed with an antibody specific for Vinculin. Densitometry was calculated using ImageJ software.

### Quantitative real-time PCR

For mRNA quantification, total RNA was isolated by using a Qiagen RNeasy kit. Using 500 ng of RNA, cDNA was synthesized by using a Verso cDNA kit (Thermo Scientific) as per the manufacturer's instructions. Analysis of mRNA levels was performed on a 7500 Fast Real-Time PCR System (Applied Biosystems) with SYBR Green-based real-time PCR. Specific primers for [KRAS F- TGACCTGCTGTGTCGAGAAT, R-TTGTGGACGAATATGATCCAA; 18S F- CGCCGCTAGAGGTGAAATTC, R-TTGGCAAATGCTTTCGCTC] were used; 18S rRNA was used as a housekeeping gene. PCR was done with reverse-transcribed RNA and 100 ng/μL of sense and antisense primers in a total volume of 20 μL. Each cycle consisted of 15 seconds of denaturation at 95°C and 1 min of annealing and extension at 60°C (40 cycles).

### Cell viability assay

Cell viability assays were performed by testing cell's ability to reduce the tetrazolium salt [3-(4,5-dimethylthiazol-2-yl)-5-(3-carboxymethoxyphenyl)-2-(4-sulfophenyl)-2H-tetrazolium, inner salt] to a formazan. Briefly, cells were seeded in a 96-well plate and were reverse transfected with either negative control siRNA, KRAS siRNA (Seq #1, Seq #2, Seq #3 or the combination of Seq #2+#3). At 24, 48, 72, 96 and 120 hours following transfection, cells were incubated with 0.15% 3-(4,5-dimethylthiazol-2-yl)-2,5-diphenyltetrazolium bromide (MTT) for 2 hours at 37°C. In the A549 experiment, 10-20 nM of siRNA was used as indicated, and in the H1299 and RMUG-S cell lines 20 nM siRNA was used. The supernatant was removed, cells were dissolved in 100 μL DMSO and the absorbance at 570 nm was recorded.

### Immunostaining

Staining was performed in formalin-fixed, paraffin embedded tumor sections (8 μm thickness) or from OCT embedded frozen tissue sections. After deparaffinization, rehydration and antigen retrieval or fixation, 3% $H_2O_2$ was used to block the endogenous peroxidase activity for 10 minutes. Protein blocking of non-specific epitopes was done using either 5% normal horse serum, 1% normal goat serum or 2.8% fish gelatin in either PBS or TBS-T for 20 minutes. Slides were incubated with primary antibody for Ki-67 (rabbit anti-mouse, 1:200, Abcam ab15580) or cleaved caspase-3 (BioCare Medical, 1:100) overnight at 4 °C. Terminal deoxynucleotidyl transferase-mediated deoxyuridine triphosphate nick-end labeling (TUNEL) staining was performed using Promega Kit (Promega, Medison, WI), and CD31 staining to assess microvessel density were performed as previously described(12, 14). For immunohistochemistry, after washing with PBS, the appropriate amount of horseradish peroxidase-conjugated secondary antibody was added and visualized with 3,3′-diaminobenzidine chromogen and counterstained with Gill's hematoloxylin #3. Light field images were obtained using a Nikon Microphot-FXA microscope and Leica DFC320 digital camera. Proliferation and apoptotic indices were determined using 6-10 representative fields at 200× magnification for each tumor, while microvessel density was determined at 100× magnification (5 tumors per group). Ki-67 and cleaved caspase-3 positive cells per high-powered field were enumerated using Cell Profiler 2.0 software, while TUNEL positive cells per high-powered field were enumerated manually(15). Quantification was performed in a blinded fashion.

### Statistical Analysis

For animal experiments, 10 mice were assigned per treatment group. This sample size provided 80% power to detect a 50% reduction in tumor mass with 95% confidence. Mouse and tumor weights and the number of tumor nodules for each group were compared using Student *t* test (for comparisons of two groups) and analysis of variance (for multiple group comparisons). For values that were not normally distributed (as determined by the Kolmogrov-Smirnov test), the Mann–Whitney rank sum test was used. A P value $\leq 0.05$ was deemed statistically significant. All statistical tests were two-sided and were performed using GraphPad Prism 6.0.

## Results

### Selection of potent KRAS siRNA sequences

To test the efficacy of KRAS silencing *in vivo*, we first searched for siRNA sequences that potently inhibit KRAS expression regardless of the specific missense mutation at codons 12, 13 or 61. Low concentrations (20 nM) of two siRNA sequences (Seq #2 and Seq #3) within the coding sequence were found to inhibit KRAS mRNA expression in mutant (A549 lung adenocarcinoma, $KRAS^{G12S}$) and wild-type (RMUG-S ovarian carcinoma) cell lines (Fig. 1A+B). Western blots further confirmed greater than 90% knock-down of KRAS protein in mutant (A549) and wild-type (H1299, RMUG-S) cancer cell lines (Fig. 1C). Compared with negative control (NC) siRNA, a single transfection of Seq #2 or Seq #3 siRNAs significantly inhibited cell viability in the A549 cell line, but not in the wild-type cells (Fig. 1D), suggesting attenuated growth is not due to off-target effects of the siRNA sequences and is consistent with A549 having a KRAS oncogene "addiction"(16). Furthermore, the combination of Seq #2 and Seq #3 at low concentrations (10 nM or 20 nM) led to substantial reductions in cell viability (Fig. 1D). As compared with H1299, KRAS siRNA sequences #2 and #3 in A549 led to marked reductions in pERK and pMEK, molecules involved in the downstream signaling of the MAPK pathway (Fig. 1E).

### Therapeutic Efficacy of KRAS siRNAs in a Lung Cancer Model

Using our well-characterized 1,2-dioleoyl-sn-glycero-3-phosphatidylcholine (DOPC) nanoliposomes (Supplementary Fig. 1)(13), we have recently demonstrated highly effective systemic delivery of oligonucleotides in orthotopic lung cancer models(12). Through exploitation of the enhanced-permeability and retention (EPR) effect(7), we also demonstrated the ability to systemically deliver siRNAs to metastatic lesions(12). Thus, for all *in vivo* experiments, we assessed therapeutic efficacy of KRAS targeting with DOPC-mediated siRNA delivery.

We first assessed whether systemically delivered KRAS siRNAs can knock-down KRAS expression *in vivo*. Four weeks following subcutaneous injection of $2.5\times10^6$ A549 cells, compared with NC siRNA, following a single injection of KRAS siRNAs Seq #2 and #3, A549 tumors had sustained knock-down of KRAS protein expression for up to 96 hours (Fig. 2A). We have previously observed similar patterns of knock-down with other targets, with rebound typically occurring around 5-6 days post-delivery(13, 17). Next, to evaluate longitudinal effects of KRAS siRNA treatment, we used luciferase-labeled A549 (A549-Luc) cells to enable IVIS imaging. Furthermore, since cisplatin (CDDP) is the backbone of lung cancer treatment, we assessed whether chemotherapy and KRAS targeting would have enhanced anti-tumor effects. In addition to primary tumors, this model demonstrated the ability to form mediastinal lymph node and chest wall metastases (Fig. 2B).

One week following orthotopic injection of $7.5\times10^5$ A549-Luc cells, mice were randomly assigned to the following treatment groups (n=10 mice/group): (1) NC siRNA-DOPC, (2) KRAS siRNA-DOPC, (3) NC siRNA-DOPC+CDDP and (4) KRAS siRNA-DOPC+CDDP. For the KRAS siRNA treatment groups, Seq #2 and Seq #3 were combined. For the CDDP treatment groups, 160 μg of CDDP was given intra-peritoneally once weekly. One week

after cell line injection, twice-weekly treatment commenced and weekly imaging was performed (Fig. 2C). Following four weeks of systemic therapy, compared to control siRNA treatment, mice in the KRAS siRNA treatment group had an 81% reduction in luminescence ($P<0.01$), while the addition of CDDP did not lead to significant reductions in the NC siRNA+CDDP or KRAS siRNA+CDDP groups (Fig. 2D+E). Longitudinal assessments of luciferase activity demonstrated significant growth inhibition from KRAS siRNA treatment (Fig. 2F), and rapid disease progression during the last week of treatment was significantly attenuated as compared with NC siRNA (Fig. 2G). Following four weeks of treatment, all mice were sacrificed and an extensive necropsy of gross tumor burden was quantified. As compared with control siRNA, significant reductions in primary tumor size (KRAS siRNA: 50%, $P=0.003$; NC siRNA+CDDP: 6%, $P=0.24$; KRAS siRNA+CDDP: 73%, $P=0.008$) and aggregate mass of distant metastases (KRAS siRNA: 77%, $P=0.0002$; NC siRNA+CDDP: 11%, $P=0.85$; KRAS siRNA+CDDP: 74%, $P=0.009$) were only observed in the KRAS siRNA treatment groups (Fig. 2H+I, Supplementary Fig. 2). The number of distant metastases was only significantly decreased in the KRAS siRNA+CDDP group (Fig. 2J). Intriguingly, only the KRAS siRNA treatment groups had significantly less frequent mediastinal metastases, while NC siRNA+CDDP did not (Fig. 2K). Taken together, systemically delivered KRAS siRNAs demonstrated significant therapeutic activity on the primary tumor as well as control of metastatic spread; while the addition of cytotoxic chemotherapy was not additive.

To further assess the biological effects of systemic KRAS siRNA treatment, we stained the tumor samples for proliferation, apoptosis and angiogenesis markers. Compared with control siRNA, significant increases in caspase-3 activity and TUNEL staining were observed in all treatment groups, with the greatest effects seen in the KRAS siRNA+CDDP group (Fig. 3A +B). Compared with control siRNA, significant reductions in Ki-67 indices were seen in all treatment groups (KRAS siRNA: 34%, NC siRNA+CDDP: 52%, KRAS siRNA+CDDP: 36%; all $P<0.0001$) (Fig. 3C). Also, compared with control siRNA, all treatment groups had significant reductions in microvessel density (KRAS siRNA: 61%, NC siRNA+CDDP: 55%, KRAS siRNA+CDDP: 76%; all $P<0.001$) (Fig. 3D). Compared with NC siRNA +CDDP, KRAS siRNA+CDDP had a 45% reduction in microvessel density ($P<0.05$, Fig. 3D). These data indicate that *in vivo* silencing of KRAS in tumors leads to induction of apoptosis and inhibition of proliferation and angiogenesis. Although the combination of KRAS siRNA with cisplatin had additive biological effects on the tumors (Fig. 3A-D), there were no appreciable effects on overall disease burden at the time of necropsy. While these findings suggest combining KRAS silencing and cisplatin may not have additive therapeutic effects, the dose chosen may have been sub-therapeutic.

## Biological Effects of KRAS siRNA in Colon Cancer Models

Next, using a recently characterized patient-derived colon cancer cell line with a $KRAS^{G12D}$ mutation(11), HCP1, we assessed whether downstream mediators of KRAS signaling are abrogated following KRAS siRNA treatment. Three weeks after early passage HCP1 subcutaneous tumors were created, mice were randomly assigned to receive a single injection of either NC siRNA-DOPC or KRAS siRNA-DOPC. Similar to before (Fig. 2C),

at both 48 and 96 hour time-points clear reductions in KRAS and pERK signaling (Fig. 4A) were observed.

Next, we assessed whether systemic KRAS siRNA could inhibit tumor growth in a colon cancer model. Following subcutaneous injection of $2.5\times10^5$ HCP1 cells, tumors were monitored until reaching approximately 100 $mm^3$. Mice were randomly assigned to the following treatment groups (n=10 mice/group): (1) NC siRNA-DOPC or (2) KRAS siRNA-DOPC. Twice weekly treatments were given and tumor volumetric assessments were made with calipers every three days. As soon as one week after treatment, significant reduction in tumor growth was noted in the KRAS siRNA-DOPC group, and following two weeks of treatment, tumors were 68.6% smaller ($P$=0.033) than the NC siRNA group (Fig. 4B).

Because the predominant site of distant metastasis in patients with colon cancer is the liver, we assessed whether KRAS siRNA would be effective in an experimental metastasis model. Splenectomy was performed one day following intra-splenic injection of $2.5\times10^5$ HCP1 cells, and mice were randomly assigned to the following groups (n=10 mice/group): (1) NC siRNA-DOPC or (2) KRAS siRNA-DOPC. As before, for the KRAS siRNA treatment groups, Seq #2 and Seq #3 were combined. Systemic treatment began 5 days following cell line injection and continued until mice in either group became moribund (22 days). Following nearly 3 weeks of treatment, KRAS siRNA led to a 73% reduction in aggregate metastatic disease ($P$=0.014, Fig. 4C) and a trend toward a reduction in the number of gross metastatic liver lesions ($P$=0.09, Fig. 4D+E). Notably, no mice in any of the therapeutic experiments exhibited any overt signs of toxicity from KRAS siRNA treatment, such as decreased feeding habits, activity, or total body weight. Taken together, systemically delivered KRAS siRNAs significantly inhibited primary tumor growth and outgrowth of distant metastases in lung and colon cancer models driven by mutant KRAS.

## Discussion

Multiple approaches have been attempted to target mutant RAS signaling, however, to date no pharmacologic inhibitors are currently in clinical use. While the ability to develop ATP-competitive inhibitors with nanomolar affinities have led to clinical efficacy(8), the low picomolar binding affinity of small GTPases for GTP and milimolar cellular concentrations of GTP make this approach far less feasible(4). Furthermore, the conformational changes following substitution of glycine (only amino acid without a side chain) for other residues in the ‘finger loop’ sterically interferes with GAP activity, making development of GAP-mimics unlikely(18). Although targeting the prenylation process of KRAS with farnesyl transferase inhibitors showed initial preclinical promise(19), enthusiasm was dampened by lack of efficacy in clinical trials(20). Most recent efforts have turned towards synthetic-lethality approaches as well as targeting of downstream signaling mediators of KRAS pathways(21, 22). Although such approaches have shown preclinical efficacy(23), compensatory mechanisms, toxicity from multiple inhibitors and ultimately efficacy in clinical trials are important hurdles that remain.

Using mutant KRAS models of lung and colon cancer, we demonstrate the therapeutic potential of systemically delivered RNAi as a novel treatment modality. While therapeutic

effects were seen through decreased downstream signaling and inhibition of proliferation, we also observed significant decreases in the frequency and burden of distant metastases. KRAS siRNA delivery as a therapeutic approach has many characteristics that make it desirable for further drug development. First, so far the first-in-human clinical trials using nanoparticle-mediated siRNA delivery have been safe, well tolerated and in some cases have led to complete pathologic responses in metastatic disease(24, 25). Second, while in this proof-of-concept study siRNA sequences which targeted all forms of mutant KRAS (and wild-type) were used, siRNA sequences that preferentially target only the mutant allele could be developed, thus theoretically avoiding toxicity from targeting the wild-type protein in normal tissues. Lastly, while other current approaches rely upon blocking the effects of mutant KRAS, whose downstream mediators consist of a highly complex circuitry, use of RNAi aims at eliminating the functional capstone, KRAS itself. While therapeutic RNAi has important challenges of its own, such as developing targeted platforms that are biocompatible and potently inhibit target expression, the field is rapidly moving forward and turning this approach into a reality(7).

## Supplementary Material

Refer to Web version on PubMed Central for supplementary material.

## Acknowledgments

The authors would like to thank Donna Reynolds for their expertise in immunohistochemistry.

**Financial Information:** Portions of this work were supported by the NIH (CA016672, CA109298, P50 CA083639, P50 CA098258, CA128797, U54 CA151668, CA177909, and U24CA143835), the CPRIT (RP110595), the Ovarian Cancer Research Fund, Inc. (Program Project Development Grant), the DOD (OC073399, W81XWH-10-1-0158), the RGK Foundation, the Gilder Foundation, the Blanton-Davis Ovarian Cancer Research Program, the Betty Anne Asche Murray Distinguished Professorship (A.K. Sood). C.V. Pecot was supported by a grant from the NCI (T32 training grant CA009666), the 2011 Conquer Cancer Foundation ASCO Young Investigator Award, the Ben F. Love Fellowship in Innovative Cancer Therapies, the Jeffrey Lee Cousins Fellowship in Lung Cancer Research and the DoCM Advanced Scholar Program. S.Y. Wu is supported by Ovarian Cancer Research Funds, Foundation for Women's Cancer, and Cancer Prevention Research Institute of Texas training grants (RP101502 and RP101489). S. Kopetz is in part supported by NIH Grant CA172670. S. Azam was supported in part by a grant from the National Institute of General medical Sciences under award 5T32 GM007092. L.M. Ellis is in part supported by NIH Grant R01CA157880, DOD CA100879 and the William C. Liedtke, Jr., Chair in Cancer Research.

## References

1. Shih C, Padhy LC, Murray M, Weinberg RA. Transforming genes of carcinomas and neuroblastomas introduced into mouse fibroblasts. Nature. 1981; 290:261–4. [PubMed: 7207618]
2. Shih C, Weinberg RA. Isolation of a transforming sequence from a human bladder carcinoma cell line. Cell. 1982; 29:161–9. [PubMed: 6286138]
3. Downward J. Targeting RAS signalling pathways in cancer therapy. Nat Rev Cancer. 2003; 3:11–22. [PubMed: 12509763]
4. Vigil D, Cherfils J, Rossman KL, Der CJ. Ras superfamily GEFs and GAPs: validated and tractable targets for cancer therapy? Nat Rev Cancer. 2010; 10:842–57. [PubMed: 21102635]
5. Hanahan D, Weinberg RA. Hallmarks of cancer: the next generation. Cell. 2011; 144:646–74. [PubMed: 21376230]
6. Fire A, Xu S, Montgomery MK, Kostas SA, Driver SE, Mello CC. Potent and specific genetic interference by double-stranded RNA in Caenorhabditis elegans. Nature. 1998; 391:806–11. [PubMed: 9486653]

7. Pecot CV, Calin GA, Coleman RL, Lopez-Berestein G, Sood AK. RNA interference in the clinic: challenges and future directions. Nat Rev Cancer. 2011; 11:59–67. [PubMed: 21160526]
8. Druker BJ, Guilhot F, O'Brien SG, Gathmann I, Kantarjian H, Gattermann N, et al. Five-year follow-up of patients receiving imatinib for chronic myeloid leukemia. The New England journal of medicine. 2006; 355:2408–17. [PubMed: 17151364]
9. Smith I, Procter M, Gelber RD, Guillaume S, Feyereislova A, Dowsett M, et al. 2-year follow-up of trastuzumab after adjuvant chemotherapy in HER2-positive breast cancer: a randomised controlled trial. Lancet. 2007; 369:29–36. [PubMed: 17208639]
10. Gupta GP, Massagué J. Cancer Metastasis: Building a Framework. Cell. 2006; 127:679–95. [PubMed: 17110329]
11. Lu J, Ye X, Fan F, Xia L, Bhattacharya R, Bellister S, et al. Endothelial cells promote the colorectal cancer stem cell phenotype through a soluble form of Jagged-1. Cancer Cell. 2013; 23:171–85. [PubMed: 23375636]
12. Pecot CV, Rupaimoole R, Yang D, Akbani R, Ivan C, Lu C, et al. Tumour angiogenesis regulation by the miR-200 family. Nature communications. 2013; 4:2427.
13. Landen CN Jr, Chavez-Reyes A, Bucana C, Schmandt R, Deavers MT, Lopez-Berestein G, et al. Therapeutic EphA2 gene targeting in vivo using neutral liposomal small interfering RNA delivery. Cancer Res. 2005; 65:6910–8. [PubMed: 16061675]
14. Shahzad MM, Lu C, Lee JW, Stone RL, Mitra R, Mangala LS, et al. Dual targeting of EphA2 and FAK in ovarian carcinoma. Cancer Biol Ther. 2009; 8:1027–34. [PubMed: 19395869]
15. Lamprecht MR, Sabatini DM, Carpenter AE. CellProfiler: free, versatile software for automated biological image analysis. Biotechniques. 2007; 42:71–5. [PubMed: 17269487]
16. Singh A, Settleman J. Oncogenic K-ras "addiction" and synthetic lethality. Cell Cycle. 2009; 8:2676–7. [PubMed: 19690457]
17. Halder J, Kamat AA, Landen CN Jr, Han LY, Lutgendorf SK, Lin YG, et al. Focal adhesion kinase targeting using in vivo short interfering RNA delivery in neutral liposomes for ovarian carcinoma therapy. Clinical Cancer Res. 2006; 12:4916–24. [PubMed: 16914580]
18. Malumbres M, Barbacid M. RAS oncogenes: the first 30 years. Nat Rev Cancer. 2003; 3:459–65. [PubMed: 12778136]
19. Kohl NE, Omer CA, Conner MW, Anthony NJ, Davide JP, deSolms SJ, et al. Inhibition of farnesyltransferase induces regression of mammary and salivary carcinomas in ras transgenic mice. Nat Med. 1995; 1:792–7. [PubMed: 7585182]
20. Sharma S, Kemeny N, Kelsen DP, Ilson D, O'Reilly E, Zaknoen S, et al. A phase II trial of farnesyl protein transferase inhibitor SCH 66336, given by twice-daily oral administration, in patients with metastatic colorectal cancer refractory to 5-fluorouracil and irinotecan. Ann Oncol. 2002; 13:1067–71. [PubMed: 12176785]
21. Barbie DA, Tamayo P, Boehm JS, Kim SY, Moody SE, Dunn IF, et al. Systematic RNA interference reveals that oncogenic KRAS-driven cancers require TBK1. Nature. 2009; 462:108–12. [PubMed: 19847166]
22. Young A, Lyons J, Miller AL, Phan VT, Alarcon IR, McCormick F. Ras signaling and therapies. Adv Cancer Res. 2009; 102:1–17. [PubMed: 19595305]
23. Engelman JA, Chen L, Tan X, Crosby K, Guimaraes AR, Upadhyay R, et al. Effective use of PI3K and MEK inhibitors to treat mutant Kras G12D and PIK3CA H1047R murine lung cancers. Nat Med. 2008; 14:1351–6. [PubMed: 19029981]
24. Davis ME, Zuckerman JE, Choi CH, Seligson D, Tolcher A, Alabi CA, et al. Evidence of RNAi in humans from systemically administered siRNA via targeted nanoparticles. Nature. 2010; 464:1067–70. [PubMed: 20305636]
25. Tabernero J, Shapiro GI, LoRusso PM, Cervantes A, Schwartz GK, Weiss GJ, et al. First-in-humans trial of an RNA interference therapeutic targeting VEGF and KSP in cancer patients with liver involvement. Cancer Discov. 2013; 3:406–17. [PubMed: 23358650]

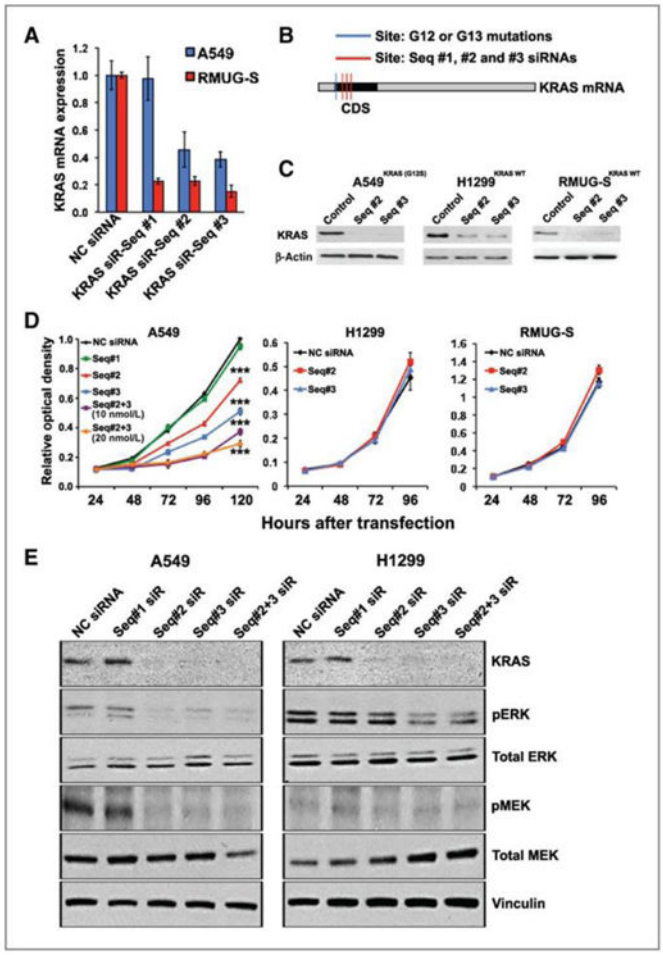


**Figure 1.**

Selection of KRAS siRNA sequences and inhibition of proliferation in a mutant cell line. (**a**) Relative knock-down of KRAS mRNA following transfection of KRAS mutant (A549; G12S) and wild-type (RMUG-S) cell lines using 20 nM siRNA. (**b**) Mature mRNA KRAS map demonstrating the binding sites of the selected KRAS siRNA Seq #1, #2 and Seq #3 (red) in relation to the region of G12 and 13 codon mutations. (Note: black designates the coding sequence, CDS). (**c**) Western blots for KRAS (top) and B-actin (bottom) 48 hours following transfection of negative control siRNA or KRAS siRNAs Seq #2 and Seq #3. (**d**) MTT viability assays following transfection of KRAS mutant and wild-type cell lines. A549 was transfected with either NC siRNA, KRAS siRNAs Seq #1, Seq#2, Seq#3 or both Seq #2 and #3 (all at 10 nM) or both Seq #2 and #3 (at 20 nM); as indicated. H1299 and RMUG-S cell lines were transfected with 20 nM of siRNA. (**e**) Western blots of A549 and H1299 cell lines 48 hours following transfection with 20 nM of the respective siRNA.

* $P < 0.05$, *** $P < 0.0001$

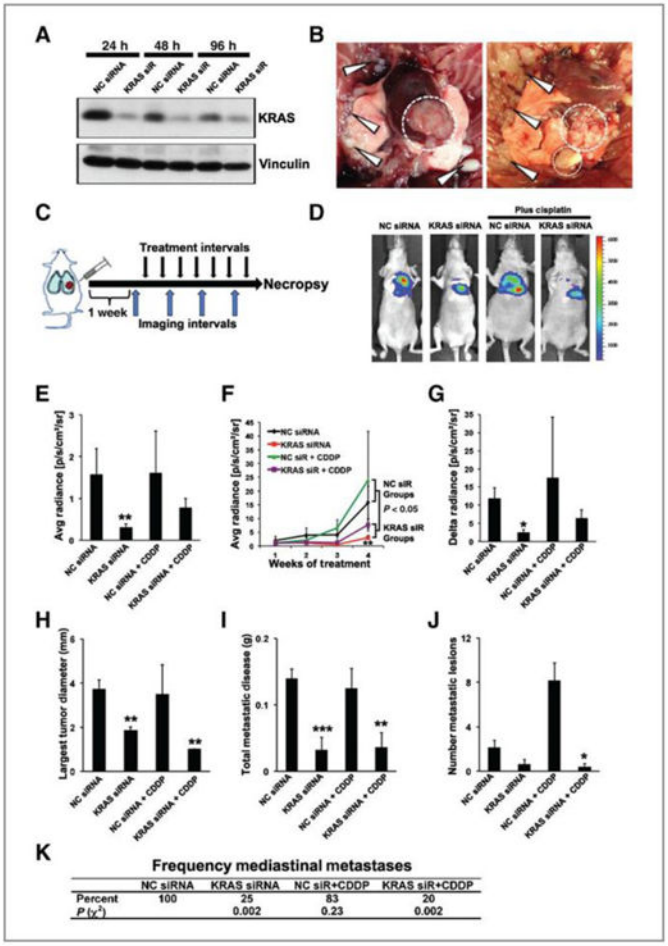


**Figure 2.**

Therapeutic efficacy of KRAS siRNA delivery in a lung cancer model. (**a**) A549 tumor expression of KRAS at 24, 48 and 96 hours following a single delivery of either NC siRNA or KRAS siRNA (Seq#2+#3), (N=3 mice/treatment group) (**b**) Representative metastatic mediastinal lymph node (dotted circle) and chest wall (white arrows) metastatic lesions of the orthotopic A549 lung cancer model. (**c**) Schematic of orthotopic A549-Luc cell line injection followed by imaging and treatment intervals. (**d**) Representative luminescent images of tumor bearing mice after the fourth week of treatment. (**e**) Average luminescence by treatment group following four weeks of treatment. (**f**) Longitudinal luminescent signals for each treatment group. (**g**) Delta of photon radiance during the last week of treatment for each treatment group. (**h**) Greatest cross-sectional dimension of the primary tumor (in mm), (**i**) total aggregate mass of metastatic burden (in grams), and (**j**) total number of metastatic lesions for each treatment group. For all experiments, each mouse received 150 μg siRNA/kg/mouse dissolved in 200 μL of PBS by the intra-peritoneal route. For the therapeutic experiment, twice weekly siRNA injections were given. Cisplatin (CDDP) was given once weekly by intra-peritoneal injection at a dose of 160 μg/mouse. N=10 mice/group, all measurements demonstrate mean ± SEM, p-values calculated using student's t-

test. (**k**) Frequency of mediastinal metastases by treatment group. P-value determined using chi-squared test.

* $P < 0.05$, ** $P < 0.01$, *** $P < 0.001$

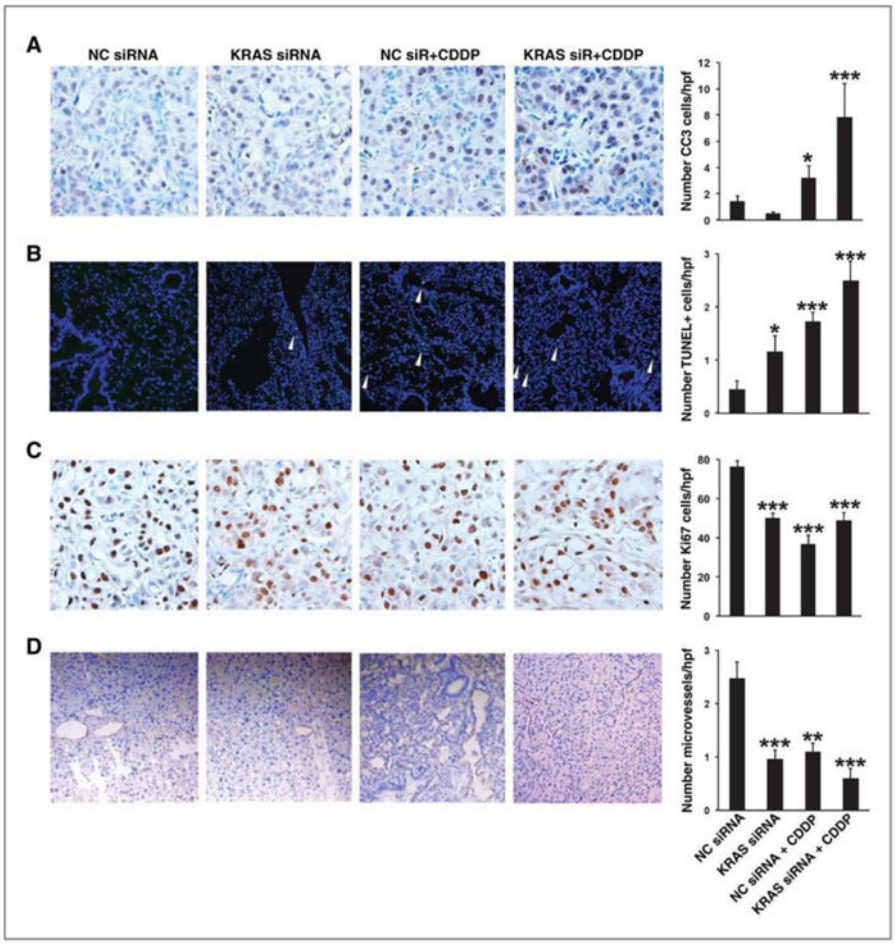


**Figure 3.**

Biological indices following KRAS siRNA and/or cisplatin treatment in a lung cancer model. (**a**) Paraffin embedded A549 tumors at the end of treatment were stained for cleaved caspase-3 or (**b**) TUNEL to assess for apoptosis. Staining for (**c**) Ki-67 was used to assess for proliferation indices. All images were taken at 200× magnification. (d) CD-31 staining was performed to assess for microvessel density (MVD). All images were taken at 100× magnification. For all biologic indices, 5-10 representative images per tumor were obtained, N=5 tumors per group. All measurements demonstrate mean ± SEM, p-values calculated using student's t-test.

* $P < 0.05$, ** $P < 0.01$, *** $P < 0.001$

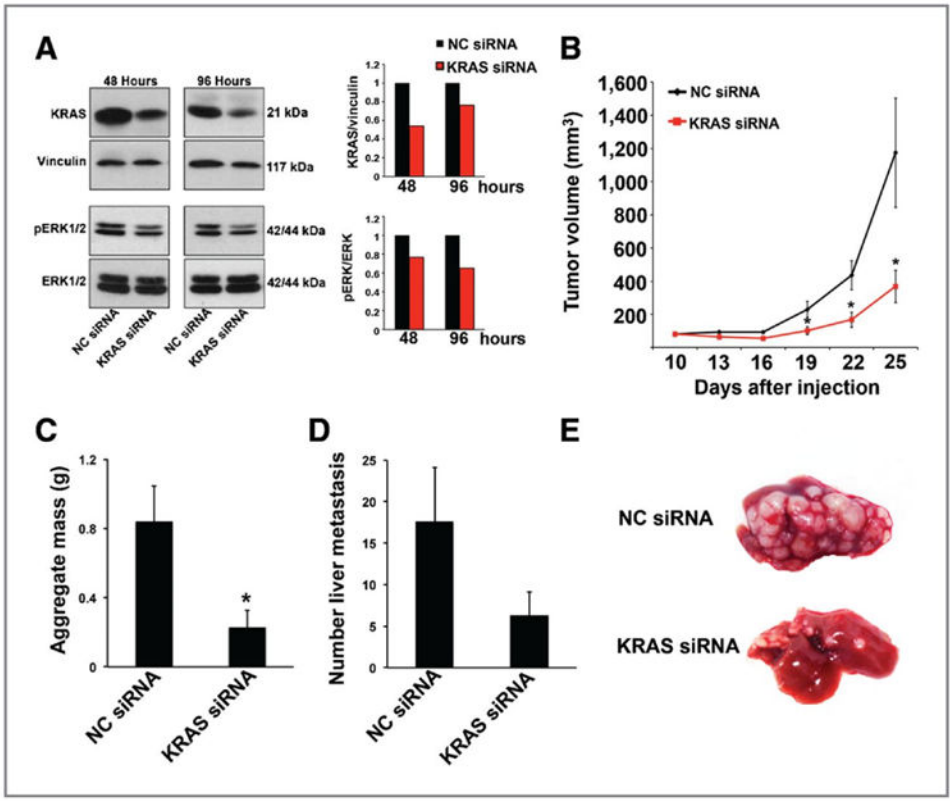


**Figure 4.**

Time-kinetics and therapeutic efficacy of KRAS siRNA in a colon cancer model. (**a**) Western blot demonstrating effects of a single KRAS siRNA treatment on KRAS protein and downstream pERK signaling 48 and 96 hours following delivery in subcutaneous HCP1 tumors, N=2 mice/treatment group. (**b**) Effects of KRAS siRNA on tumor growth in a colon cancer model (HCP1) based on tumor volume. (**c**) Following injection of HCP1 cells into the spleen, mice were randomized and assigned to either NC siRNA or KRAS siRNA (Seq #2 and #3) treatment. Following approximately 3 weeks of treatment, aggregate burden of metastatic disease and (**d**) total number of liver metastases was assessed. (**e**) Representative tumors from NC siRNA and KRAS siRNA treatment groups demonstrating liver metastases at time of necropsy. N=10 mice/group, all measurements demonstrate mean ± SEM, p-values calculated using student's t-test.

* $P < 0.05$